Simulation of Adaptive Control Applied on Tubular Chemical Reactor

JIRI VOJTESEK, PETR DOSTAL
Department of Process Control, Faculty of Applied Informatics
Tomas Bata University in Zlin
nám. T. G. Masaryka 5555, 760 01 Zlin
CZECH REPUBLIC
{vojtesek,dostalp}@fai.utb.cz

Abstract: - Simulation has a big importance nowadays when the speed of computers grows rapidly and the price is on the other hand decreasing. The paper is focused on the simulation of the steady-state and dynamic behaviour of the nonlinear system represented by the tubular chemical reactor with the co-current and counter-current cooling in the jacket. These analyses are then used for the choice of the suitable control strategy. The adaptive controller used here is based on the choice of the External Linear Model as a linear representation of the originally nonlinear system parameters of which are identified recursively. The polynomial method together with spectral factorization and pole-placement method used in control synthesis satisfies the basic control requirements. The resulted hybrid controller provides good control results although the system has strongly nonlinear behaviour.

Key-Words: - Tubular chemical reactor, Adaptive control, Recursive identification, Polynomial approach, External Linear Model

1 Introduction

Tubular chemical reactor is tool frequently used in chemical industry for production of the several chemicals. From the mathematical point of view This type of reactor belongs to the class of systems with distributed parameters Chyba: zdroj odkazu nenalezen from the mathematical point of view. Configuration with one main pipe with several pipes inside used in this work offers cooling in the remaining space of the main pipe with the same or opposite direction to the flow direction of the reactant. The direction of the cooling could be with the same direction as the flow of the reactant (co-current) or with the opposite direction (counter-current). One task of this contribution will be focused on the comparison of these two cooling techniques from the efficiency point of view.

Controlling of such processes with conventional methods with fixed parameters of the controller could be problem mainly in the cases where the working point changes. This inconvenience should be overcome with the use of some of "new" control strategies such as adaptive control, predictive control etc. This work show process of the designing of the adaptive controller [3]. The adaptation is process known from the animals and plants which adapts their behaviour to the environment. This process means the loss of the energy collects information and experiences about the system.

Adaptive approach here is based on the choice of the External Linear Model (ELM) of originally nonlinear system, parameters of which are estimate recursively and parameters of the controller are recomputed in each step according these identified ones.

The delta models [4] were used in ELM. Although these models belongs to the class of discrete-time models, parameters of such models approaches to the continuous-time ones for small sampling period [5].

The polynomial approach together with the pole-placement method [6] which are used for the designing of the controller satisfy basic control requirements such as stability, disturbance attenuation or reference signal tracking.

The adaptive control is not the only one so called "modern" control method which can be used for these types of reactors. Classical PI or PID controllers which can be used are shown in [7], the use of the Smith predictors is in [8] and the robust control in [9].

All methods were verified by simulations in the mathematical simulation software Matlab, version 6.5. The next will be connected with the verification on the real plant which is necessary due to reliability of the simulation results.

2 Nonlinear System

The nonlinear system under the consideration is represented by the tubular chemical reactor with simple exothermic reaction A → B → C [10]. Mathematical description of such process is very complex and so we introduce some simplifications. We neglect heat losses and conduction along the metal wall of the pipes, but heat transfer through the wall is consequential for a dynamic study. Furthermore, we expect that all densities, heat capacities and heat transfer coefficients are constant.

This type of chemical reactor provides two options for cooling from the direction point of view – (I.)co-current and (II.)counter-current cooling. The graphical representation of the tubular chemical reactor with both co- and counter-current cooling can be found in Fig. 1 and Fig. 2.

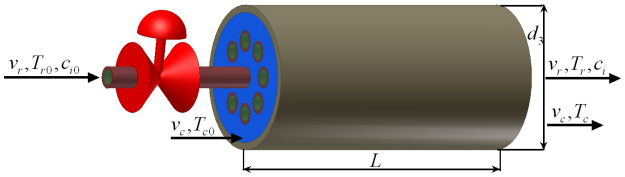

Fig. 1 Tubular chemical reactor with co-current cooling in the jacket

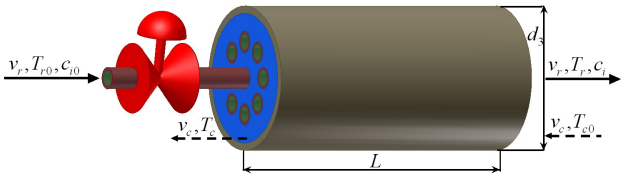

Fig. 2 Tubular chemical reactor with counter-current cooling in the jacket

The reactor has one big pipe and several individual pipes with the flowing reactant inside. Detail of one individual pipe inside the tubular reactor is displayed in Fig. 3.

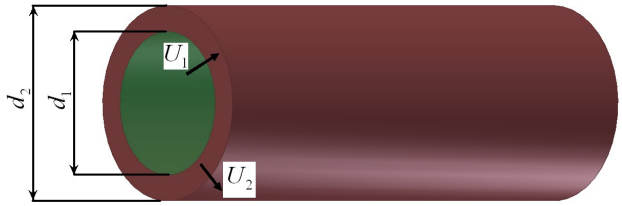

Fig. 3 Individual pipe of the tubular chemical reactor

2.1 Mathematical Model

The mathematical model is in this case described by the set of five PDE derived from the balances inside the reactor:

$$\frac{\partial c_A}{\partial t} + v_r \cdot \frac{\partial c_A}{\partial z} = -k_1 \cdot c_A \tag{1}$$

$$\frac{\partial c_B}{\partial t} + v_r \cdot \frac{\partial c_B}{\partial z} = k_1 \cdot c_A - k_2 \cdot c_B \tag{2}$$

$$\frac{\partial T_r}{\partial t} + v_r \cdot \frac{\partial T_r}{\partial z} = \frac{Q_r}{\rho_r \cdot c_{rp}} - \frac{4 \cdot U}{d_1 \cdot \rho_r \cdot c_{pr}} \cdot \left(T_r - T_w\right) \tag{3}$$

$$\frac{\partial T_w}{\partial t} = \frac{4 \cdot \left[d_1 U_1 \left(T_r - T_w\right) + d_2 U_2 \left(T_c - T_w\right)\right]}{\left(d_2^2 + d_1^2\right) \cdot \rho_w \cdot c_{pw}} \tag{4}$$

These four PDE are common for both co- and counter-current cooling. The difference can be found in the last PDE which comes from the heat balance of the cooling liquid.

This equation has for co-current cooling form:

$$\frac{\partial T_c}{\partial t} + v_c \cdot \frac{\partial T_c}{\partial z} = \frac{4 \cdot n_1 \cdot d_2 \cdot U_2 \cdot \left(T_w - T_c\right)}{\left(d_3^2 - n_1 \cdot d_2^2\right) \cdot \rho_c \cdot c_{pc}} \tag{5}$$

and for counter-current cooling:

$$\frac{\partial T_c}{\partial t} - v_c \cdot \frac{\partial T_c}{\partial z} = \frac{4 \cdot n_1 \cdot d_2 \cdot U_2 \cdot \left(T_w - T_c\right)}{\left(d_3^2 - n_1 \cdot d_2^2\right) \cdot \rho_c \cdot c_{pc}} \tag{6}$$

where T is the temperature, d represents diameters, ρ are densities, c_p means specific heat capacities, U stands for the heat transfer coefficients, n_1 is a number of tubes and L represents the length of the reactor. Index $(\bullet)_r$ means the reaction compound, $(\bullet)_w$ is for the metal wall of the pipes and $(\bullet)_c$ for the cooling liquid. Variables v_r and v_c are fluid velocities of the reactant and cooling liquid, respectively, as

$$v_r = \frac{q_r}{f_r}; \quad v_c = \frac{q_c}{f_c} \tag{7}$$

where q are flow rates and f are constants

$$f_r = n_1 \cdot \frac{\pi \cdot d_1^2}{4}; \quad f_c = \frac{\pi}{4} \cdot \left(d_3^2 - n_1 \cdot d_2^2\right) \tag{8}$$

The reaction velocities, k_i, in equations (1) - (2) and equations are nonlinear functions of the temperature computed via the Arrhenius law:

$$k_j = k_{0j} \cdot \exp \frac{-E_j}{R \cdot T_r}, \text{ for } j = 1,2 \tag{9}$$

where k_{0j} represents pre-exponential factors, E means activation energies and R is a gas constant. Q_r in the equation (3) is reaction heat computed as

$$Q_r = h_1 \cdot k_1 \cdot c_A + h_2 \cdot k_2 \cdot c_B \tag{10}$$

and h_j is used for reaction enthalpies.

The mathematical model shows that this plant is *a nonlinear system with continuously distributed parameters*. Strong nonlinearity can be found in Equation (3), and the system is with distributed parameters because of the presence of the PDE

where the state variable is related not only to the time variable, t, but the space variable, z, too.

In this case the initial conditions are $c_A(z,0) = c_A^s(z)$, $c_B(z,0) = c_B^s(z)$, $T_r(z,0) = T_r^s(z)$, $T_w(z,0) = T_w^s(z)$ and $T_c(z,0) = T_c^s(z)$ and boundary conditions $c_A(0,t) = c_{A0}(t)$, $c_B(0,t) = c_{B0}(t) = 0$, $T_r(0,t) = T_{r0}(t)$ and $T_c(\mathrm{L},\mathrm{t}) = T_{cL}(t)$.

Fixed parameters of the reactor [10] are shown in the Table 1.

2.2 Steady-state and Dynamic Analyses

The steady-state and dynamic analyses usually precede the design of the controller because they help with the understanding of the system's behaviour.

Name of the parameter	Symbol and value of the parameter
Inner diameter of the pipe	$d_1 = 0.02\ m$
Outer diameter of the pipe	$d_2 = 0.024\ m$
Diameter of the jacket	$d_3 = 1\ m$
Number of pipes	$n_1 = 1200$
Length of the reactor	$L = 6\ m$
Density of the reactant	$\rho_r = 985\ kg.m^3$
Density of the pipe's wall	$\rho_w = 7800\ kg.m^3$
Density of the cooling	$\rho_c = 998\ kg.m^3$
Heat capacity of the reactant	$c_{pr} = 4.05\ kJ.kg^{-1}.K^{-1}$
Heat capacity of the pipe's wall	$c_{pw} = 0.71\ kJ.kg^{-1}.K^{-1}$
Heat capacity of the cooling	$c_{pc} = 4.18\ kJ.kg^{-1}.K^{-1}$
Heat transfer coefficient: reactant-wall	$U_1 = 2.8\ kJ.m^{-2}.K^{-1}.s^{-1}$
Heat transfer coefficient: wall-cooling liquid	$U_2 = 2.56\ kJ.m^{-2}.K^{-1}.s^{-1}$
Pre-exponential factor for reaction 1	$k_{10} = 5.61\times10^{16}\ s^{-1}$
Pre-exponential factor for reaction 2	$k_{20} = 1.128\times10^{16}\ s^{-1}$
Activation energy of react.1/ R	$E_1/R = 13477\ K$
Activation energy of react.2 /R	$E_2/R = 15290\ K$
Enthalpy of reaction 1	$h_1 = 5.8\times10^4\ kJ.kmol^{-1}$
Enthalpy of reaction 2	$h_2 = 1.8\times10^4\ kJ.kmol^{-1}$
Input concentration of A	$c_{A0}^s = 2.85\ kmol.m^{-3}$
Input temperature of the reactant	$T_{r0}^s = 323\ K$
Input temperature of the cooling	$T_{c0}^s = 293\ K$

Table 1: Fixed parameters of the reactor

From the mathematical point of view, the static analysis means solving of the set of PDE (1) - (5) for the time close to infinity, which means that all derivatives with respect to time are equal to zero.

The position derivatives can be replaced easily by the first forward differences, i.e.

$$\left.\frac{dx}{dz}\right|_{z=z_0} \approx \frac{x(i)-x(i-1)}{h_z}$$
$$\left.\frac{dx}{dz}\right|_{z=z_0} \approx \frac{x(j+1)-x(j)}{h_z} \qquad (11)$$

where x is a general variable, h_z is an optional size of the step in axial direction, $i = 1, 2, \ldots, n$ and $j = n, n\text{-}1, \ldots, 0$. The defined input boundary conditions, x_0, for $i = 1$ are equal to boundary conditions $x(0)$. If the reactor is divided into N_z equivalent parts, the discretization step is

$$h_z = \frac{L}{N_z} \qquad (12)$$

where L denotes the length of the reactor and $N_z = 100$.

The steady-state analysis was examined for various values of volumetric flow rate of the cooling in the range $q_c^s = \langle 0.1;\ 0.35\rangle\ [m^3.s^{-1}]$ and 3D results for both co-current and counter-current cooling in the jacket and throughout the length of the reactor represented by the variable z $[m]$ on the y-axis are shown in Fig. 4 to Fig. 7. These graphs clearly shows high nonlinearity of the system.

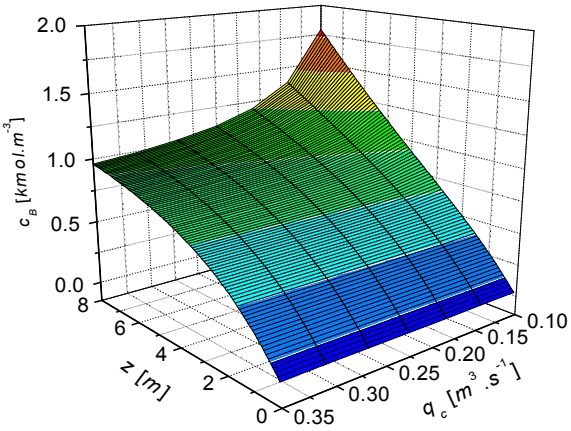

Fig. 4 Steady-state analysis of c_B^s for different volumetric flow rate of cooling q_c, co-current cooling

The steady-state analysis also results in the optimal working point. The optimal working point is a combination of input variables which provides the most efficient, stable, save or least expensive results. The working point here cannot be found

clearly and it is defined by the volumetric flow rate of the reactant $q_r^s = 0.150\ m^3.s^{-1}$ and the volumetric flow rate of the coolant $q_c^s = 0.275\ m^3.s^{-1}$.

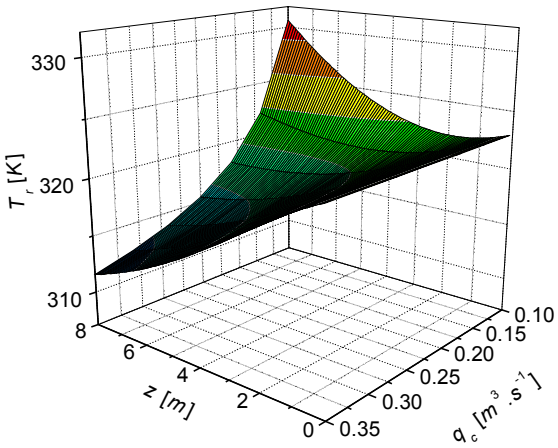

Fig. 5 Steady-state analysis of T_r^s for different volumetric flow rate of cooling q_c, co-current cooling

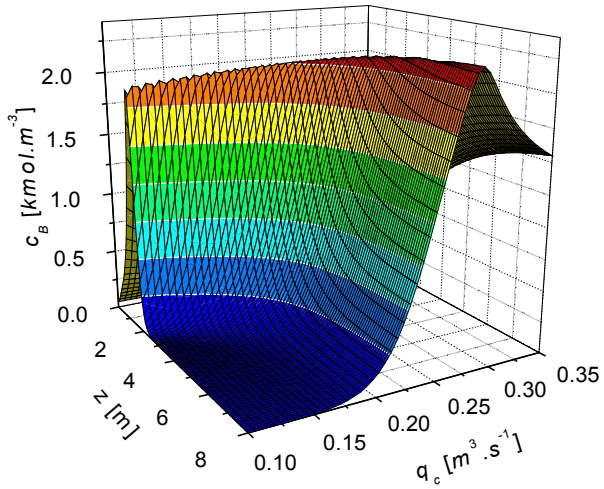

Fig. 6 Steady-state analysis of c_B^s for different volumetric flow rate of cooling q_c, counter-current cooling

The second, dynamic, analysis examines the behaviour after the step change of one of the input variables. Because the set of PDE (1) - (5) includes again derivatives with the respect to axial variable z, the discretization (12) must be used. The set of PDE is then transformed to a set of ODE which is then solved by the standard Runge-Kutta's method.

Although there are several input variables, the dynamic analysis here was done for different step changes of the volumetric flow rate of the cooling liquid, Δq_c^s. Output variables $y_1(t)$ and $y_2(t)$ illustrate the difference between the actual values of the c_B and T_r at the end of the reactor ($z = L$) and its steady-state value c_B^s or T_r^s respectively. Mathematically speaking, there input and output variables are described as

$$u(t)=\frac{q_c(t)-q_c^s}{q_c^s}\cdot 100[\%]$$
$$y_1(t)=c_B(t,L)-c_B^s[kmol.m^{-3}] \quad (13)$$
$$y_2(t)=T_r(t,L)-T_r^s[K]$$

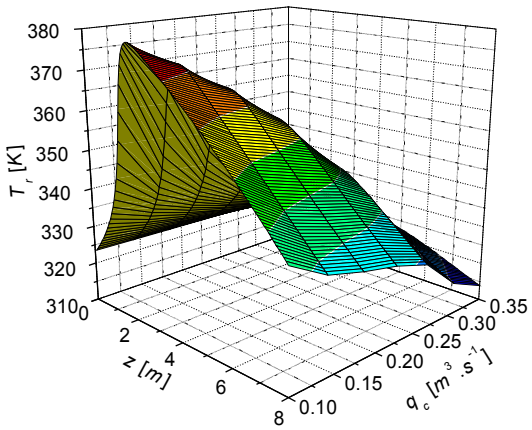

Fig. 7 Steady-state analysis of T_r^s for different volumetric flow rate of cooling q_c, counter-current cooling

There were done two dynamic analyses both output variables $y_1(t)$ and $y_2(t)$ and for four values of the input change of volumetric flow rate of the coolant Δq_c^s = -20%, -10%, 10% and 20%. The first analysis observes dynamic behaviour for co-current and results are shown in Fig. 8 and Fig. 9.

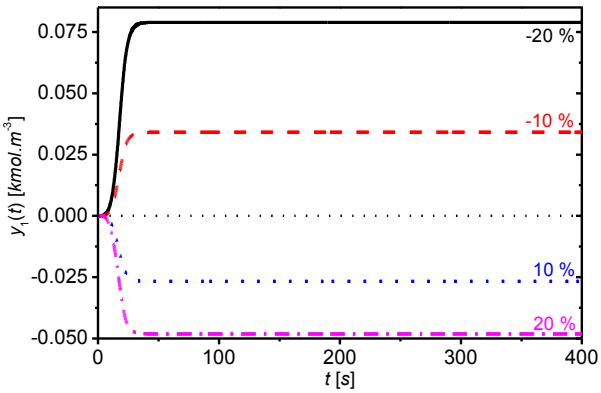

Fig. 8 Output responses of output $y_1(t)$ for various step changes Δq_c^s and co-current cooling

Both results show relatively smooth course and they could be replaced by the first or the second order transfer function for the control purposes.

The second dynamic analysis was done for the same step changes of input volumetric flow rate of

the coolant Δq_c^s as in the previous case. The results are shown in Fig. 10 and Fig. 11. Very interesting is the course of the output $y_1(t)$ which represents change of the product's concentration c_B. This output shows typical non-minimum phase behaviour and time delay. On the other hand, the output $y_2(t)$ could be replaced by the first or the second order transfer function.

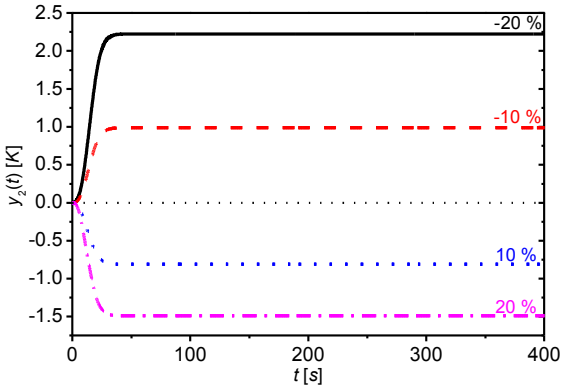

Fig. 9 Output responses of output $y_2(t)$ for various step changes Δq_c^s and co-current cooling

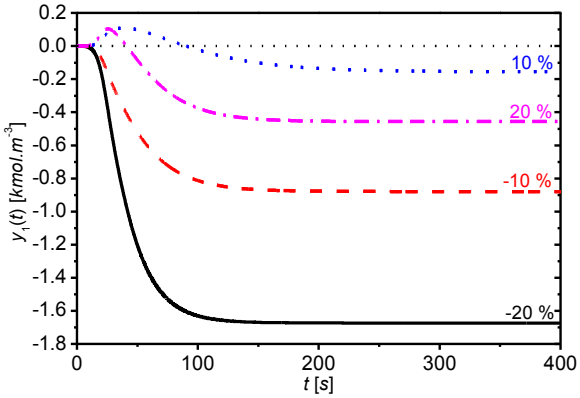

Fig. 10 Output responses of output $y_1(t)$ for various step changes Δq_c^s and counter-current cooling

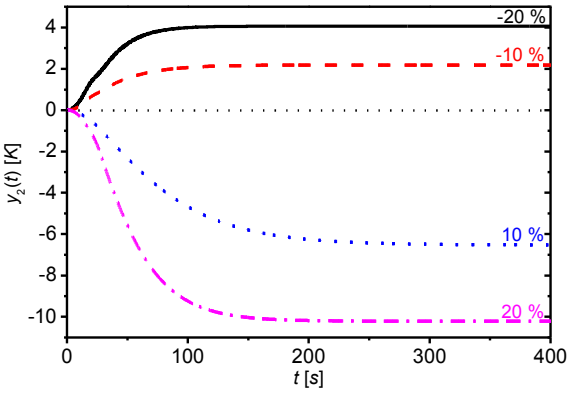

Fig. 11 Output responses of output $y_2(t)$ for various step changes Δq_c^s and counter-current cooling

Previous analyses have shown dynamic behaviour of the reactor for both co-current and counter-current cooling. The comparison of these cooling techniques is shown in the following pictures.

The first two graphs in Fig. 12 and Fig. 13 for the step change Δq_c^s = 20% clearly presents bigger efficiency of the counter-current cooling.

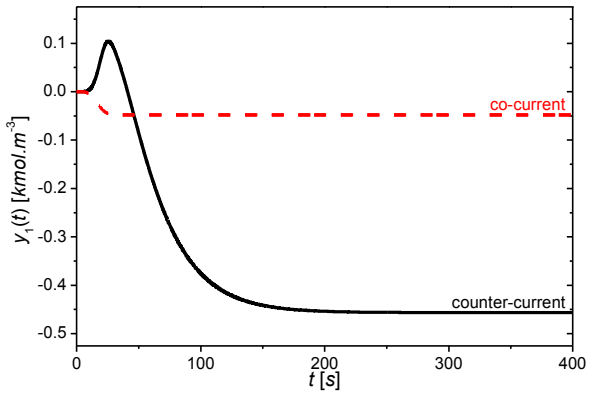

Fig. 12: Comparison of co- and counter-current cooling for the step change Δq_c^s = 20% and output $y_1(t)$

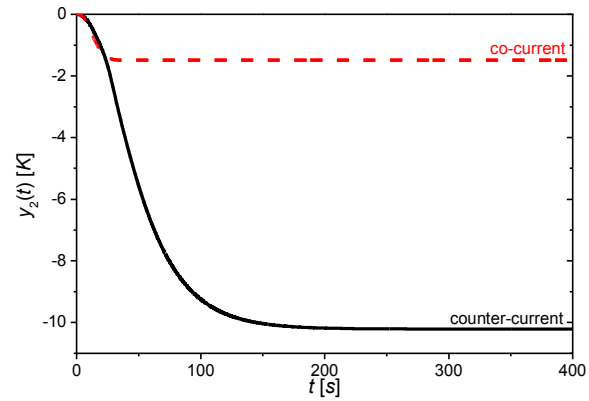

Fig. 13 Comparison of co- and counter-current cooling for the step change Δq_c^s = 20% and output $y_2(t)$

The second comparison was done for the step change -20% of the input volumetric flow rate of the cooling, i.e. Δq_c^s.

The co-current cooling in the jacket has again nearly two times better cooling efficiency for the the same input step change according to the co-current cooling for the output temperature of the coolant which is hidden in the variable $y_2(t)$. Surprising result can be found in Fig. 14, where the product's concentration c_B (i.e. $y_1(t)$) runs in positive values unlike the negative values for the counter-current cooling.

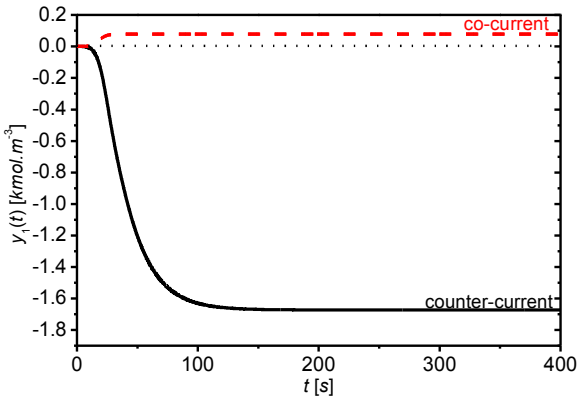

Fig. 14 Comparison of co- and counter-current cooling for the step change Δq_c^s = -20% and output $y_1(t)$

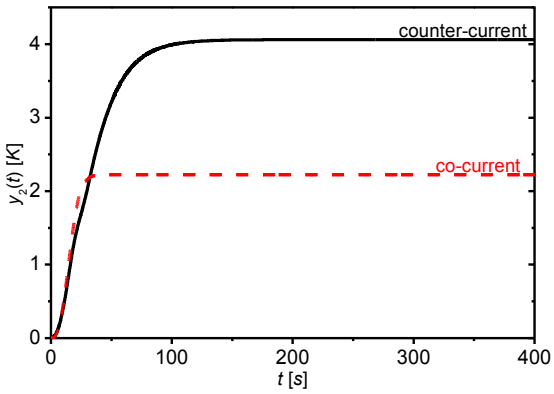

Fig. 15 Comparison of co- and counter-current cooling for the step change Δq_c^s = -20% and output $y_2(t)$

The dynamic analyses results in the choice of the control input and controlled output which are in our case the change of the volumetric flow rate of the coolant (Δq_c^s) as an input and the change of the temperature of the reactant at the end of reactor ($y_1(t) \rightarrow T_r(t,Z)$) as a controlled output. Mathematically speaking, input and output variables in the next graphs means:

$$u(t)=\frac{q_c(t)-q_c^s}{q_c^s}\cdot 100\,[\%]$$
$$y(t)=T_r(t,L)-T_r^s\,[K] \qquad (14)$$

The decision which cooling strategy will be used was relatively simple – simulations have proven that the counter-current cooling has better cooling efficiency and it was chosen as for the cooling of the exothermic reaction inside the reactor.

Dynamic responses displayed in Fig. 11 show that this output should be expressed by the first or the second order transfer function, e.g.

$$G(s)=\frac{b(s)}{a(s)}=\frac{b_0}{a_1 s+a_0}$$
$$G(s)=\frac{b(s)}{a(s)}=\frac{b_1 s+b_0}{a_2 s^2+a_1 s+a_0} \qquad (15)$$

Previous experiences have shown that the most suitable is the choice of the second order transfer function with relative order one which could deal with the possible non-minimum phase behaviour.

Due to the simplification, the parameter a_2 will be later on set to $a_2 = 1$, i.e.

$$G(s)=\frac{b(s)}{a(s)}=\frac{b_1 s+b_0}{s^2+a_1 s+a_0} \qquad (16)$$

3 Adaptive Control

The adaptive approach here is based on the recursive parameter identification of the ELM (16) which represents originally nonlinear system and parameters of the controller are recomputed according to the estimated parameters in every step too [3].

The controller is designed via polynomial synthesis [6] which fulfils basic control requirements such as stability, reference signal tracking, disturbance attenuation and it can be used for systems with negative control properties. The control configuration with one degree-of-freedom (1DOF) is displayed in Fig. 16.

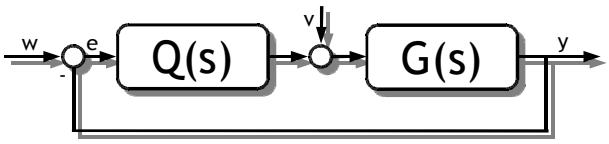

Fig. 16 1DOF control configuration

Block Q in Fig. 16 represents the transfer function of the controller, G denotes the transfer function (16) of the plant, w is the reference signal, e is used for the control error, v is the disturbance at the input to the system, u determines the input variable, and finally y is the output variable. Polynomials $a(s)$ and $b(s)$ in the transfer function (14) are commensurable polynomials in complex s-plane. The feasibility condition is fulfilled if the system is proper, i.e. deg $a(s) \geq$ deg $b(s)$.

The transfer function of the controller then is

$$\tilde{Q}(s)=\frac{q(s)}{s\cdot\tilde{p}(s)} \qquad (17)$$

where polynomials $q(s)$ and $\tilde{p}(s)$ are computed from the Diophantine equation

$$a(s)\cdot s\cdot\tilde{p}(s)+b(s)\cdot q(s)=d(s) \qquad (18)$$

by the method of uncertain coefficients which compares coefficients of individual *s*-powers. The polynomial $d(s)$ on the right side of (18) is stable optional polynomial which fulfills the stability of the controller.

Degrees of the polynomials $q(s)$,a $\tilde{p}(s)$ and $d(s)$ are for the transfer function (14)

$$\begin{aligned}\deg\tilde{p}(s)&\geq\deg a(s)-1=1\\ \deg q(s)&=\deg a(s)=2\\ \deg d(s)&=\deg a(s)+\deg\tilde{p}(s)+1=4\end{aligned} \tag{19}$$

which means that the transfer function of the controller in Equation (17) could be rewritten to form

$$\tilde{Q}(s)=\frac{q_2 s^2+q_1 s+q_0}{s\cdot(p_1 s+p_0)} \tag{20}$$

The optional polynomial $d(s)$ is in our case

$$d(s)=m(s)\cdot n(s) \tag{21}$$

where $m(s)$ is $m(s)=(s+\alpha)^2$ for $\alpha > 0$ and $n(s)$ comes from the spectral factorization of $a(s)$:

$$\begin{aligned}n^*(s)\cdot n(s)&=a^*(s)\cdot a(s)\\ n_0&=\sqrt{a_0^2}\\ n_1&=\sqrt{a_1^2+2n_0-2a_0}\end{aligned} \tag{22}$$

Polynomials $a(s)$ and $b(s)$ in (16), (18) and (22) are known from the recursive identification.

The previous synthesis was derived for the continuous-time (CT) models. The problem with the CT models can be found in the on-line identification which is much more complicated than the identification of the discrete-time (DT) models. This inconvenience could be solved for example by the use of differential filter.

In our case, delta (δ–) models were used for the estimation model. Although the delta models belong to the class of discrete-time models, parameters of such model approach to the continuous-time model for small sampling period which was proofed for example in [5].

The δ–model introduces a new complex variable γ computed as (see [4]):

$$\gamma=\frac{z-1}{\beta\cdot T_v\cdot z+(1-\beta)\cdot T_v} \tag{23}$$

where β is a parameter from the interval $0 \leq \beta \leq 1$ and T_v means a sampling period. It is clear that we can obtain infinite number of δ–models for various β. A so called forward δ-model for $\beta = 0$ was used and γ operator is then

$$\gamma=\frac{z-1}{T_v} \tag{24}$$

The continuous model (16) is then rewritten to the form

$$a^\delta(\delta)y(t')=b^\delta(\delta)u(t') \tag{25}$$

where polynomials $a^\delta(\delta)$ and $b^\delta(\delta)$ are discrete polynomials and their coefficients are different from those of the CT model $a(s)$ and $b(s)$.

The transfer function $G(s)$ in (16) could be rewritten to the form of differential equation:

$$\begin{aligned}y_\delta(k)=&-a_1^\delta y_\delta(k-1)-a_0^\delta y_\delta(k-2)+\dots\\ &+b_1^\delta u_\delta(k-1)+b_0^\delta u_\delta(k-2)\end{aligned} \tag{26}$$

which is in the vector form

$$y_\delta=\boldsymbol{\theta}_\delta^T(k)\cdot\boldsymbol{\varphi}_\delta(k-1) \tag{27}$$

and the vector of the parameters, $\boldsymbol{\theta}_\delta$, and the data vector, $\boldsymbol{\varphi}_\delta$, are then

$$\begin{aligned}\boldsymbol{\theta}_\delta(k)&=\left[a_1^\delta, a_0^\delta, b_1^\delta, b_0^\delta\right]^T\\ \boldsymbol{\varphi}_\delta(k-1)&=\left[-y_\delta(k-1), -y_\delta(k-2)\dots\right.\\ &\left.\dots, u_\delta(k-1), u_\delta(k-2)\right]^T\end{aligned} \tag{28}$$

$$\begin{aligned}y_\delta(k)&=\frac{y(k)-2y(k-1)+y(k-2)}{T_v^2}\\ y_\delta(k-1)&=\frac{y(k-1)-y(k-2)}{T_v}\\ y_\delta(k-2)&=y(k-2)\\ u_\delta(k-1)&=\frac{u(k-1)-u(k-2)}{T_v}\\ u_\delta(k-2)&=u(k-2)\end{aligned} \tag{29}$$

The goal of the identification is to estimate vector of parameters $\boldsymbol{\theta}_\delta$ in ARX model (27) from the previous values of the input and output variables in the time intervals remote by sampling period T_v.

The recursive least-squares method with exponential forgetting was used for identification in this work. This method could be simply described by the set of equations:

$$\begin{aligned}\varepsilon(k)&=y(k)-\boldsymbol{\varphi}^T(k)\cdot\hat{\boldsymbol{\theta}}(k-1)\\ \gamma(k)&=\left[1+\boldsymbol{\varphi}^T(k)\cdot\boldsymbol{P}(k-1)\cdot\boldsymbol{\varphi}(k)\right]^{-1}\\ \boldsymbol{L}(k)&=\gamma(k)\cdot\boldsymbol{P}(k-1)\cdot\boldsymbol{\varphi}(k)\\ \boldsymbol{P}(k)&=\frac{1}{\lambda_1(k-1)}\dots\\ \dots&\left[\boldsymbol{P}(k-1)-\frac{\boldsymbol{P}(k-1)\cdot\boldsymbol{\varphi}(k)\cdot\boldsymbol{\varphi}^T(k)\cdot\boldsymbol{P}(k-1)}{\frac{\lambda_1(k-1)}{\lambda_2(k-1)}+\boldsymbol{\varphi}^T(k)\cdot\boldsymbol{P}(k-1)\cdot\boldsymbol{\varphi}(k)}\right]\\ \hat{\boldsymbol{\theta}}(k)&=\hat{\boldsymbol{\theta}}(k-1)+\boldsymbol{L}(k)\cdot\varepsilon(k)\end{aligned} \tag{30}$$

where exponential forgetting factor λ_1 is constant course which is described via

$$\lambda_1(k)=1-K\cdot\gamma(k)\cdot\varepsilon^2(k) \tag{31}$$

and K is very small value, in our case the value was chosen to $K = 0.001$. Previous equations are easily programmable in the MATLAB.

4 Simulation Results

Proposed control strategies were verified by the simulation in the mathematical software MATLAB. Due to most comparable results, all simulations were done for time T_f = 10 000 *s* and five different step changes ($w(t)$ = 4.5, -1.5, 2.5, -3 and 4 *K*) every 2 000 *s* were simulated during this time.

The sampling period was T_v = 1.5 *s*, the starting vector of parameters for the on-line identification was $\boldsymbol{\theta}_{\boldsymbol{\delta}}(0)=[0.1, 0.1, 0.1, 0.1]^T$ and and the covariance matrix $\boldsymbol{P}$ has 1x10^7 on the diagonal.

The controller could be tuned via choice of parameter α and three control analyses were done for α = 0.007, 0.01 and 0.02. The results are shown in the following figures.

Simulation results displayed in Fig. 17 and Fig. 18 clearly shows that the increasing value of the parameter α results in quicker output response but overshoots especially if the the value of the reference signal $w(t)$ jumps from the higher value to the lower one. Jumps from lower value to the higher has generally much better responses. The highest value of α, i.e.α = 0.021 also generates much quicker and shaking changes of the input variable $u(t)$ (see Fig. 18) which is not very good from the practical point of view while this variable represents the twist of the valve and rapid changes could influence the vitality of the valve.

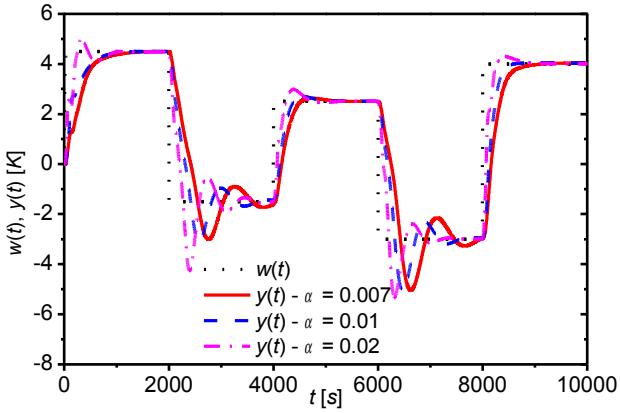

Fig. 17: The course of the output variable $y(t)$ for various α

The quality of the control is qualified with the control quality criteria S_u and S_y computed as

$$S_u=\sum_{i=St}^{N}\left(u(i)-u(i-1)\right)^2[-]; \qquad \text{for } N=\frac{T_f}{T_v} \qquad (32)$$

$$S_y=\sum_{i=St}^{N}\left(w(i)-y(i)\right)^2[K^2];$$

where *St* is starting time of the computation which is in this case due to inaccurate identification at the very beginning after the second step change in time 2 000 *s*, i.e. St = 2000/T_v. The results for all three simulations are shown in Table 2.

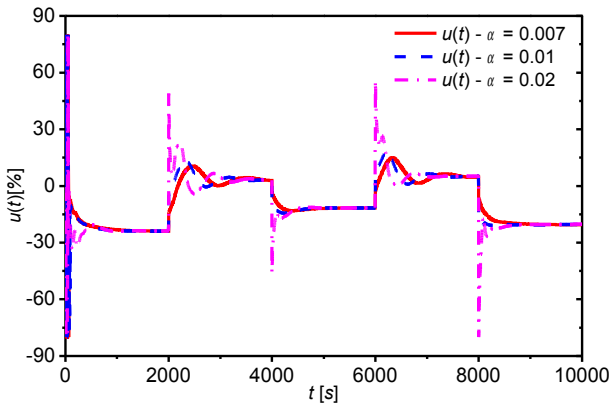

Fig. 18 The course of the input variable $u(t)$ for various α

	S_u [-]	S_y [K^2]
α = 0.007	335	16 077
α = 0.01	5 012	9 130
α = 0.02	22 425	7 547

Table 2 Control quality criteria S_u and S_y

This table clearly shows, that the control configuration with α = 0.02 has the best results from the output point of view (criterion S_y). On the other hand, the controller with α = 0.007 has the best results for the input (S_u) which is important from the practical point of view. We can say that the choice of the optimal value of a is depends on the what is more important from the control point of view – the reference tracking and speed or the most attentive course of the input variable.

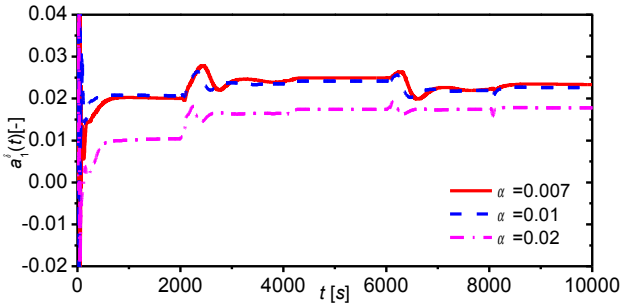

Fig. 19 The course of the identified parameter a_1^{δ} for various α

The course of the identified parameters $a_1^{\delta}, a_0^{\delta}, b_1^{\delta}, b_0^{\delta}$ shown in Fig. 19 - 22 also shows usability of this control method. The only problem

with the identification could be found at the very beginning of the control when the controller does not have enough information about the plant because the estimated vector starts from the general form $\boldsymbol{\theta}_{\boldsymbol{\delta}}(k)=[0.1, 0.1, 0.1, 0.1]^T$. On the other hand, the step changes does not provide such problems and estimation to the new variables is very quick.

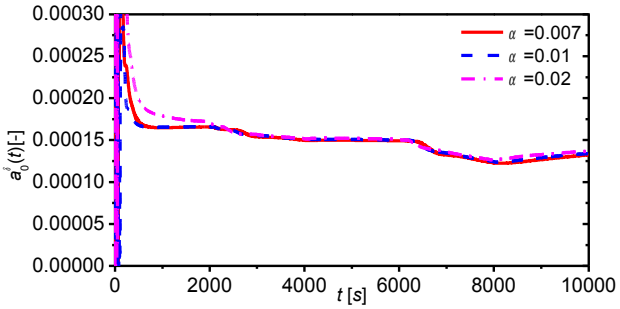

Fig. 20 The course of the identified parameter a_0^{δ} for various α

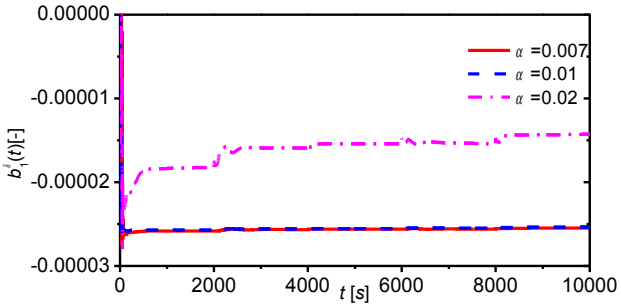

Fig. 21 The course of the identified parameter b_1^{δ} for various α

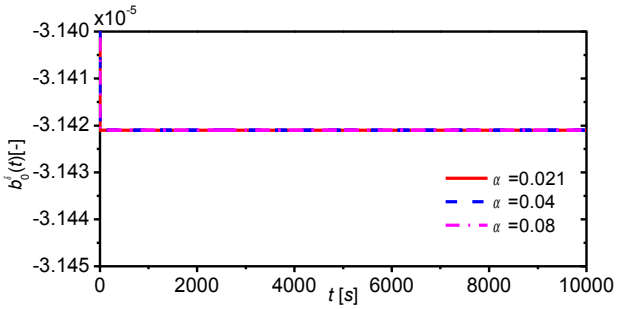

Fig. 22 The course of the identified parameter b_0^{δ} for various α

As written in the theoretical part, the nominated adaptive controller can deal with disturbance attenuation, which is proved in Fig. 23 and Fig. 24.

The simulation time was 10 000 *s* and the value of criterion α was equal to 0.008. Three disturbances are injected to the system: $v_1(t)$ = +1.5% step change of the input concentration c_{A0} for time t = <3 000, 10 000> *s*, $v_2(t)$ = 0.25 *K* step change of the input temperature T_{r0} for time t = <5 000, 10 000> *s* and $v_3(t)$ = -0.2 *K* step change of the output temperature T_r for time t = <7 000, 10 000> *s*.

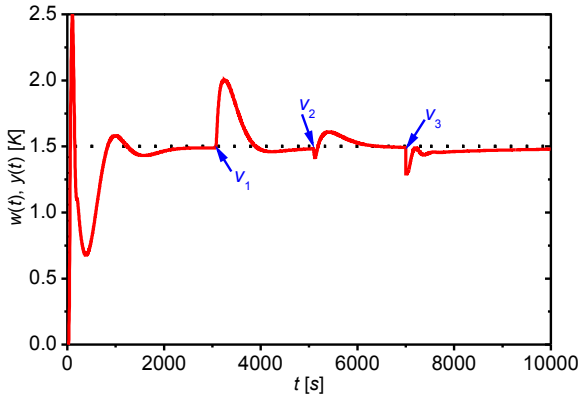

Fig. 23 The course of reference $w(t)$ and output variable $y(t)$ for three disturbances, α = 0.008

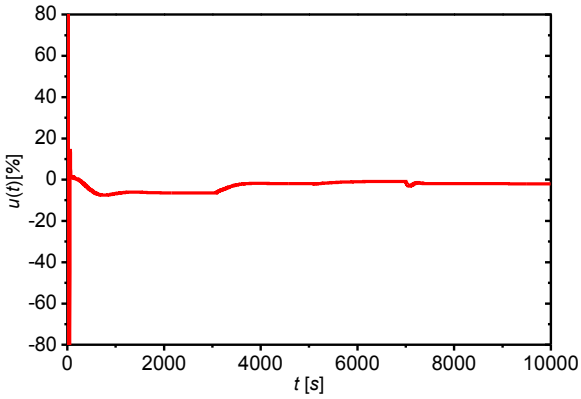

Fig. 24 The course of the input variable $u(t)$ for three disturbances, α = 0.008

The course of the output variable shows that the proposed controller has no problem to deal with these three disturbances. One small problem could be found again at the very beginning of the control, due to identification of the ELM. The adaptive controller, similarly as in previous control studies stars from the general values of the vector of the parameters. Please note that each disturbance affects the controller from its starting time, i.e. 3 000, 5 000 and 7 000 *s* to the end of the simulation time interval (10 000 *s*) which means that all three disturbances operate together at the last time interval from 7 000 to 10 000 *s* and the controller has still very good control results. The values of control quality criteria computed from (32) are S_u = 30 382.23 and S_y = 284.03.

5 Conclusion

This paper is focused on the procedure from the modelling and simulation of the steady-state and dynamics of the nonlinear system to the adaptive control of this system.

The nonlinear process here is represented by the tubular chemical reactor which belongs to the range of the systems with continuously distributed parameters. The static analysis shows, as we expected, nonlinear behaviour of the system.

The dynamic analysis point out mainly better cooling efficiency of the counter-current cooling in this type of plug-flow reactors. These analyses also helps with the choice of the ELM used later in the adaptive control. The second order transfer function with relative order one was used as a linear representation of the originally nonlinear system.

The use of polynomial synthesis together with the pole-placement method allows the controller could be tuned via position of the root α. It was proofed that the increasing value of this parameter results in quicker output response but bigger overshoots. On the other hand, lower values of α provides more smoother courses of the input variable $u(t)$ which is also important from the practical point of view because this variable is in this case represented by the valve in the cooling pipe. Quick changes of the volumetric flow rate could practically destroy the valve.

Although this system has nonlinear behaviour, the proposed controller provides good control results and it can be used for controlling such processes. The next step should be verification on the real plant.

References:

[1] J. Ingham, I. J.Dunn, E. Heinzle, J. E. Přenosil, *Chemical Engineering Dynamics*. An Introduction to Modelling and Computer. Simulation. Second, Completely Revised Edition, VCH Verlagsgesellshaft, Weinheim, 2000.

[2] J. Vojtěšek, P. Dostál, R. Matušů, Effect of Co- and Counter-current Cooling in Tubular Reactor, In: *Proc. 7th International Scientific-Technical Conference Process Control 2006*. Kouty n. Desnou. Czech Republic, 2006.

[3] V. Bobál, J. Böhm, J. Fessl, J. Macháček, *Digital Self-tuning Controllers: Algorithms, Implementation and Applications.* Advanced Textbooks in Control and Signal Processing. Springer-Verlag London Limited, 2005.

[4] S. Mukhopadhyay, A. G. Patra, G. P. Rao, New class of discrete-time models for continuous-time systems, *International Journal of Control*, vol.55, 1161-1187,1992.

[5] D. L. Stericker, N. K. Sinha, "Identification of continuous-time systems from samples of input-output data using the δ-operator". *Control-Theory and Advanced Technology*, vol. 9, 113-125, 1993.

[6] V. Kučera, Diophantine equations in control – A survey" *Automatica*, 29, 1361-1375, 1993.

[7] Matušů, R., Prokop, R.: Experimental Verification of Design Methods for Conventional PI/PID Controllers. *WSEAS Transactions on Systems and Control*, Vol. 5, No. 5, 2010, pp. 269- 280, ISSN 1991-8763.

[8] Matušů, R., Prokop, R.: Control of Periodically Time-Varying Systems with Delay: An Algebraic Approach vs. Modified Smith Predictors. *WSEAS Transactions on Systems*, Vol. 9, No. 6, 2010, pp. 689-702, ISSN 1109-2777.

[9] Matušů, R., Prokop, R., Matejičková, K., Bakošová, M.: Robust Stabilization of Interval Plants using Kronecker Summation Method. *WSEAS Transactions on Systems*, Vol. 9, No. 9, 2010, pp. 917-926, ISSN 1109-2777.

[10] P. Dostál, R. Prokop, Z. Prokopová, M. Fikar, Control design analysis of tubular chemical reactors. *Chemical Papers*, 50, 195-198, 1996.